Recent Results of Seismic Isolation Study in CRIEPI
-Numerical Activities-

Hiroo SHIOJIRI, Dr.Eng, Katsuhiko ISHIDA Dr.Eng,
Shuichi YABANA, Kazuta HIRATA,
Abiko Research Laboratory, Central Research Institute
of Electric Power Industry.

1. Introduction

Development of detailed numerical models of a bearing and the related isolation system is necessary for establishing the rational design of the bearing and the system.

The developed numerical models should be validated regarding the physical parameters and the basic assumption by comparing the experimental results with the numerical ones.

The numerical work being conducted in CRIEPI consists of the following items.

(1) Simple modeling of the behavior of the bearings capable of approximating the tests on bearings, and the validation of the model for the bearing by comparing the numerical results adopting the models with the shaking table tests results.

(2) Detailed three-dimensional modeling of single bearings with finite-element codes, and the experimental validation of the model.

(3)Simple and detailed three-dimensional modelings of isolation buildings, and, experimental validations.

The results of the numerical work obtained so far are described here.

2. Simple modeling of bearings

(1) Modeling

The nonlinear characteristics of bearings were determined from an engineering point of view so as to meet the values of both equivalent stiffness(Keq) and equivalent viscous damping ratio(Heq) which were calculated based on the results of the preliminary element tests. Fig.1 shows how to determine the bilinear characteristics from the restoring loops obtained in the preliminary bearing tests using this engineering method. Bilinear models which give both Keq and Heq as obtained from the preliminary element tests results must meet the following conditions.

The primary curve of the bilinear hysteresis loop must pass point C shown in Fig.2-1, which corresponds to a specified target displacement δ d, so that this bilinear primary curve gives a target Keq.

The points on the primary curve of the bilinear hysteresis loop must correspond to a set of yielding shear displacement δ y and yielding shear Qy in order for the area

enclosed by the bilinear loop △W to be the same as that obtained from the bearing test results, so that this bilinear hysteresis loop gives a target Heq.

In these relationships, numerous of yielding horizontal displacement δy and yielding shear force Qy which give the specified value of △W could exist on a line A-B which is parallel to line O-C as shown in Fig.2-1. To select one particular set of δy and Qy, a loop fitting method was used in this study. In this method, the sum of square of differences between the assumed bilinear loop and the loop obtained in the test results(solid circular marks in Fig2-3) was calculated at selected values of δy in a range of 0 to δd and the one which gives the least value for the sum of square of differences was selected for δy in the bilinear primary curve. In this study, the displacement δd was determined to be the maximum displacement of the bearing recorded in the shaking table test.

Four different types of nonlinear model were used in the simulation analyses (see Fig.2.2)

① Bilinear model: the model properties can be determined by the method described above. This model gives the required Heq solely by hysteretic damping, therefore, this model has no damping for the displacement less than δy.

② Bilinear + linear model: LRB consists of laminated rubber bearing and lead plug. To consider the internal viscous damping of laminated rubber bearing in the analysis model. This model consists of the linear visco-elastic model with the equivalent Keq and Heq of laminated rubber bearing alone and the bilinear model which represents the nonlinear characteristics of lead plug. The bilinear model were calculated by subtracting linear stiffness and equivalent hysteresis area corresponding to elastmeric rubber bearing from the bilinear model defined in ①.

③ Overlay model: The bilinear model described in ① gives the target Keq and Heq for a specified displacement amplitude. The Overlay model was obtained by combining several bilinear models so that it gives target △W's and Keq's for several different displacement amplitudes. As an example of overlay model, Keq and Heq calculated from the bearing test results of LRB, and the nonlinear characteristics of a set of shear springs whose combination produces a overlay model were shown in Table 2-1 and Table2-2, respectively. Furthermore, Fig.2-3 shows the hysteresis loops calculated by the overlay model of HRB subjected to gradually increasing displacement steps.

④ Nonlinear Elastic + Damper model: It is known that Heq of HRB has dependence on displacement amplitude. In this model, the nonlinear elastic characteristics which give Keq for several different displacement amplitudes were combined with the viscous damper which gives Heq for a specified displacement amplitude δd.

(2) Validation by Shaking Table Tests

The outline of the analytical model for one directional excitation is shown in Fig.2.2. The steel frame of superstructure and the isolation layer(bearings) were modeled by shear-flexural beam elements, and a nonlinear shear with a linear rocking spring, respectively. The isolation layer of the test specimen was composed of a set of nine bearing. The modeling of bearings are discussed above. The isolation layer was modeled by a single nonlinear shear spring and a single linear rocking spring that represent characteristics of 9 bearings.

Three types of modeling method were applied for each type of bearings which was tested on the shaking table. The maximum displacements of bearings recorded in the shaking table tests and the target displacements δ d, as used for modeling were shown in Table 2-3. It should be noted that in the analysis cases of A-3 or C-3 a overlay model was used for different input earthquake levels. Fig.2-5 shows the time histories recorded in the tests and analytical results for comparison. The analytical results show a good agreement with the test results in both response acceleration and displacement waveforms. However, in the test results, the acceleration responses at RF and 1F levels contain some high frequency components. The maximum acceleration distribution and the floor response spectra at 2F level(corresponding to the reactor location in an actual plant) of the model with LRB subjected to S1 level earthquake input are shown in Fig.2-6 and Fig.2-7, respectively. The results by the analytical model which gives the specified Keq and Heq at the amplitude around the maximum displacement recorded in the shaking table test show a good agreement with the test results. As for the floor response spectra, the maximum peak values and the overall shapes of peak obtained from the analyses are in a good agreement with the test results in the period range from 0.1 sec. to 1.0. sec where the first mode of the isolation system becomes dominant. The maximum acceleration distributions and the floor response spectra for the model with HRB under S1 level earthquake input are shown in Fig.2-8 and Fig.2-9, respectively. As for the maximum acceleration distribution, the results of the analysis case B-2 show the best agreement with the test results. In the comparison of floor response spectra, the analytical results of all three analysis cases show a good agreement with the test results in the range from 0.1sec to 1.0sec. The hysteresis loop of LRB and HRB isolation layers under S1 level earthquake input are shown in Fig.2-10 and Fig.2-11, respectively Although there is a tendency that the maximum displacements of analyses are slightly smaller than those of test results, agreements between the analytical results and the test results are regarded to be satisfactory. The maximum acceleration distribution and the floor response spectra of the model with LRB subjected to 1.5S1 level earthquake input are shown in Fig.2-12 and Fig.2-13, respectively. As input earthquake level increases, differences among the analytical results with different modeling methods become noticeable, in particular, in the floor

response spectra.

The results of the analytical case C-3 which used an overlay model are in good agreements with the test results for both the maximum displacement distribution and the floor response spectra. The hysteresis loops of LRB isolation layer subjected to 1.5S1 level earthquake input are shown in Fig.2-14. The maximum displacement of the analytical case C-1 which used a bilinear model is smaller than the corresponding test value.

The uni-directional nonlinear models were extended to the two-dimensional horizontal nonlinear models by using Multiple Shear Spring (MSS) method. Simulation of the test model with LRB for multi-directional inputs of S1 level earthquake were performed. The concept of MSS is shown in Fig.2-15. The nonlinear properties of each direction used in this model is the same as those of the analytical case A-2. Fig.2-16 shows the relative horizontal displacement orbit of bearings. The analytical results properly simulated the behavior of bearings in the horizontal plane as observed in the shaking table test.

(3) Summary of results

The analytical results are in a good agreement with the test results in case of S1 level earthquake input for the first mode response, in which the deformation of the isolation layer was dominant. Therefore, the adequacy of modeling methods for nonlinear properties was confirmed. An overlay model can adequately simulate the test results of different input earthquake levels, i.e., S1 and 1.5S1.

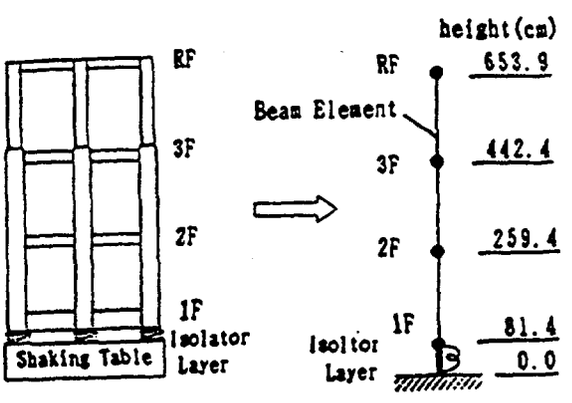

Fig.2-4 Analytical Modeling

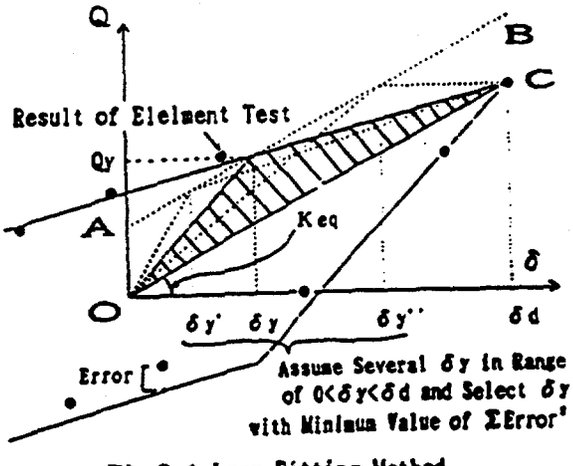

Fig.2-1 Loop Fitting Method

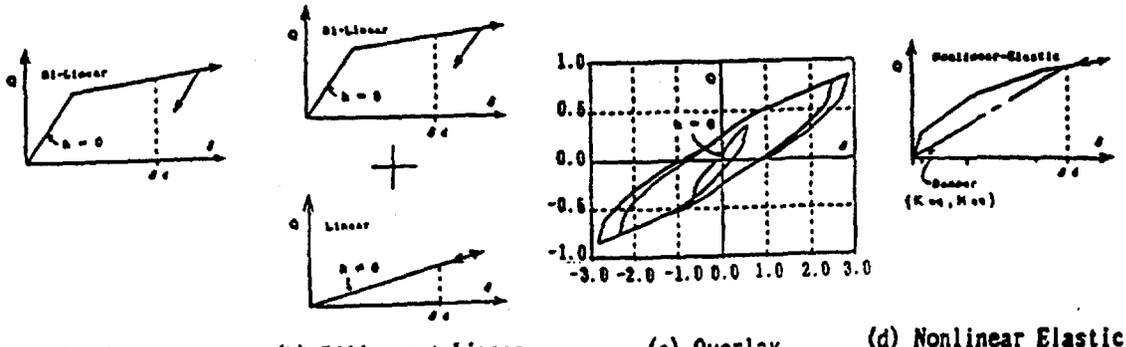

(a) Bilinear (b) Bilinear + Linear (c) Overlay (d) Nonlinear Elastic + Damper

Fig.2-2 Types of Nonlinear Properties used in Analyses

Table.2-1 Element Test Results

HORIZONTAL STRAIN γ (%)	HORIZONTAL DISPL. δ (cm)	Keq (ton/cm)	heq (%)
25	0.375	0.629	14.57
50	0.750	0.542	13.33
100	1.500	0.428	11.93
150	2.250	0.363	10.63

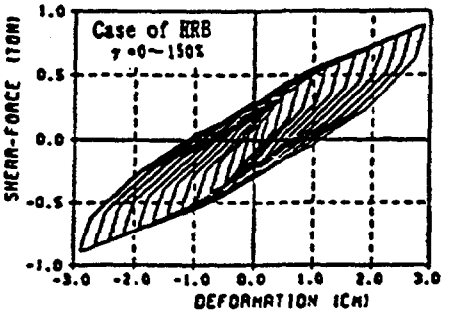

Fig.2-3 Example of Overlay Model

Table.2-2 Nonlinear Properties of Overlay Model Component

STIFFSESS CHANGING POINT(cm)	NON-LINEAR ELASTIC (ton/cm)	BI-LINEAR (1) (ton/cm)	BI-LINEAR (2) (ton/cm)	BI-LINEAR (3) (ton/cm)	BI-LINEAR (4) (ton/cm)	TOTAL STIFFSESS (ton/cm)
0.051*	2.499	11.090	1.292	0.471	0.078	15.350
0.375	2.302	0.000	↑	↑	↑	4.143
0.750	3.546	↑	0.000	↑	↑	4.095
1.500	2.746	↑	↑	0.000	↑	2.825
	2.097	↑	↑	↑	0.000	2.097

*The 1st stiffness changing point was calculated by hysteresis loop fitting of horizontal strain of 25%

Table.2-3 Analytical Cases

TEST CASE	ISOLATOR	INPUT LEVEL	MAXIMUM DISPL. (TEST:cm)	ANALYTICAL CASE	TYPE OF ANALYSIS MODEL	DISPLACEMENT USED TO DETERMIN MODEL PROPERTIES (cm)
A	LRB	S1	[1.13, 1.07]	A-1	(a)Bi-linear	] 0.750
				A-2	(b)Bi-linear + Linear	
				A-3	(c)Overlay*	0.375, 0.750, 1.50, 2.25
B	HRB	S1	[0.93, 0.87]	B-1	(a)Bi-linear	] 0.966
				B-2	(d)Nonlinear Elastic + Damper	
				B-3	(c)Overlay	0.483, 0.966, 1.93, 2.90
C	LRB	1.5S1	[1.73, 1.72]	C-1	(a)Bi-linear	] 1.50
				C-2	(b)Bi-linear + Linear	
				C-3	(c)Overlay*	0.375, 0.750, 1.50, 2.25

*Analytical case A-3 and C-3 use same analysis property model.

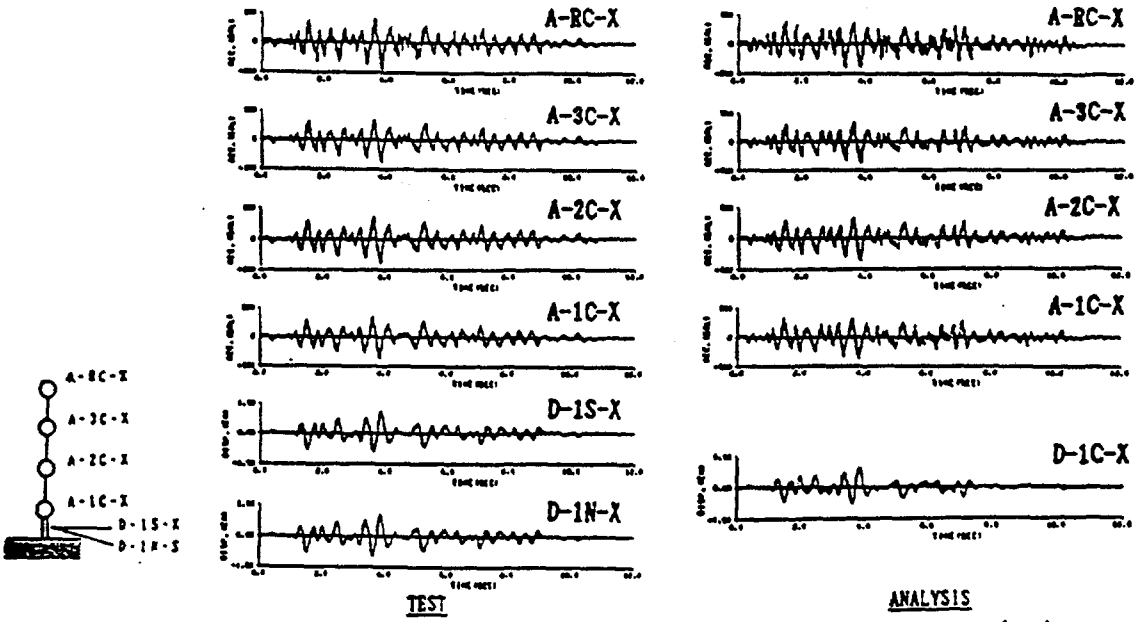

Fig.2-5 Waveforms of Test Results and Analytical Results(A-2)

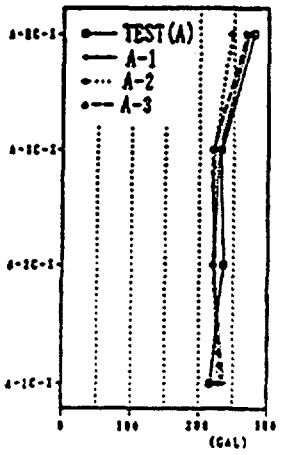

Fig.2-6 Maximum Acceleration Profiles(LRB:S1)

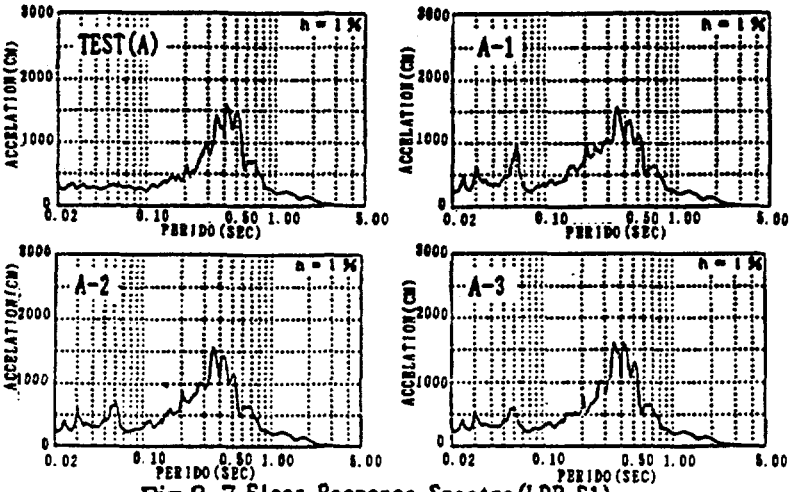

Fig.2-7 Floor Response Spectra(LRB:S1)

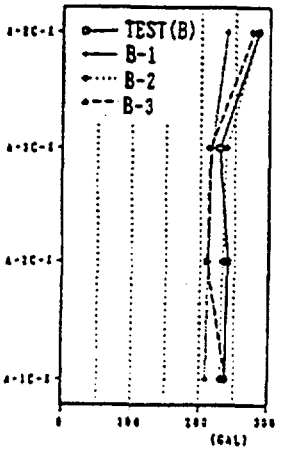

Fig.2-8 Maximum Acceleration Profiles(HRB:S1)

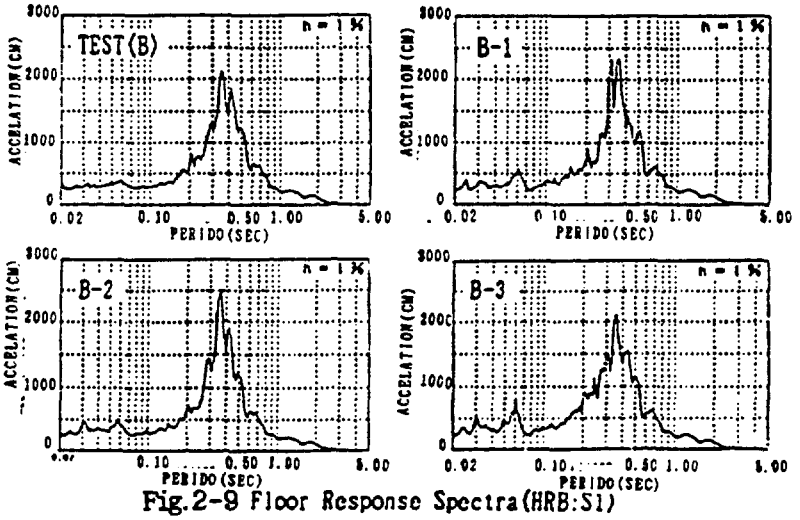

Fig.2-9 Floor Response Spectra(HRB:S1)

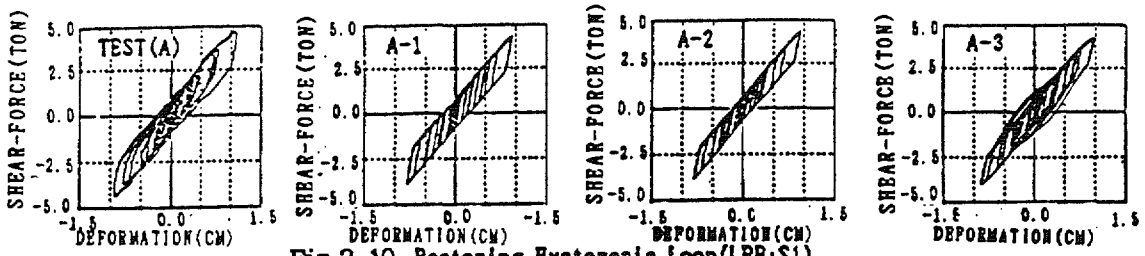

Fig.2-10 Restoring Hysteresis Loop(LRB:S1)

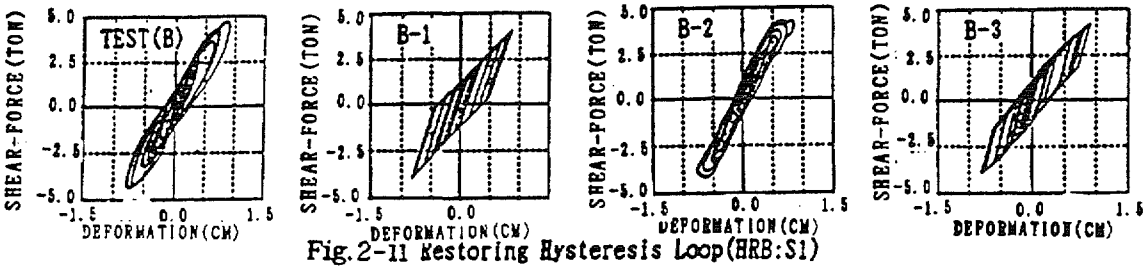

Fig.2-11 Restoring Hysteresis Loop(HRB:S1)

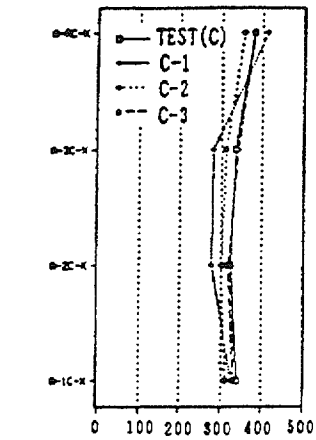

Fig2-12 Maximum Acceleration Profiles(LRB:1.5S1)

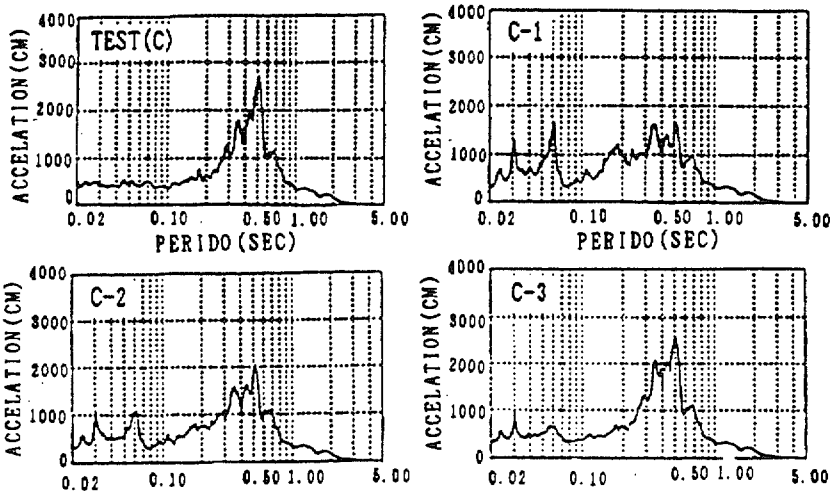

Fig.2-13 Floor Response Spectra(LRB:1.5S1)

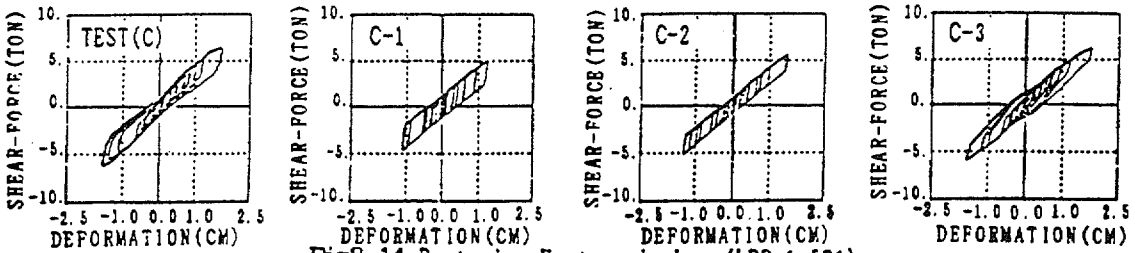

Fig2-14 Restoring Hysteresis Loop(LRB:1.5S1)

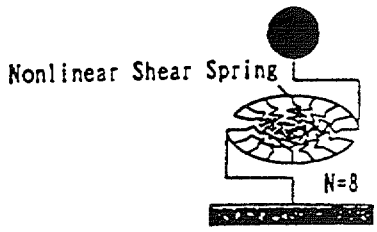

Fig.2-15 MSS Model

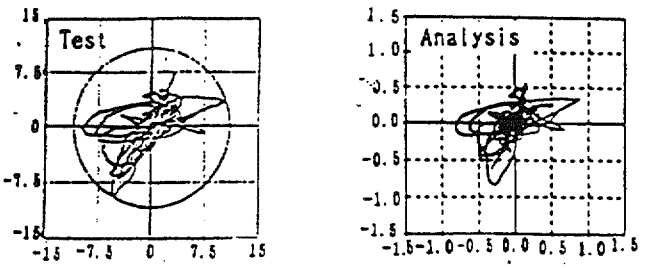

Fig.2-16 Orbits of Isolator Layer

3. Three-Dimensional Modeling of Single Bearing

(1) Numerical Model

The numerical method for the bearing must be able to handle geometrical and materia nonlinearities, since maximum strain of rubber can be as much as several hundred percent and elastic modulus are strain dependent.

General purpose finite element programs MARC and ABAQUS have such capabilities and were applied to the analysis of the bearings. For simplicity, rubber is assumed to be isotropic, hyperelastic and nearly incompressible. Element type used in the analysis by MARC and ABAQUS are listed in Table 3-1.

Constitutive equations used were as follows.

Model A (Mooney Rivlin Model)

$$W = C_{10}(I_1 - 3) + C_{01}(I_1 - 3) \tag{1}$$

Where,

$$I_1 = \lambda_1^2 + \lambda_2^2 + \lambda_3^2$$
$$I_2 = \lambda_1^2\lambda_2^2 + \lambda_2^2\lambda_3^2 + \lambda_1^2\lambda_3^2$$
$$I_3 = \lambda_1^2\lambda_2^2\lambda_3^2$$
$$I_3 = 1$$

W=energy density function, and

W = energy density function,
and $\lambda_i\ (i=1,2,3)$ = the principal extension ratios.

Coefficients of Eq.(1) were determined to fit the shear test of rubber bearing.

Model B

$$\frac{\partial W}{\partial I_1} = a_i + b_i(I_1 - 3) + c_i(I_1 - 3)^2 + d_i \exp\{e_i(I_1 - 3)\} \tag{2}$$

Coefficients of Eq.(2) were determined to fit the bi-axial test of rubber material (Fig.3-1)

(2) Simulation of Laminated Elastomer Bearing

1) Laminated Elastomer bearing and FE mesh.

The bearing which support 4.9×10^3N(500t_g)of weight were simulated. At first, vertical load was applied, and then forced horizontal displacement was given to the upper flange. Considering the symmetry of the geometry of the bearing, loadings, and displacements, only a half of the bearing was modeled. Linear hexahedral elements were used for steel plate and rubber.

The number of meshes in circumferential direction and in radial direction were 8 and 2, respectively. Each rubber sheet or steel plate is divided into two meshes in thickness direction. The number of layers were 25. FEM mesh is shown in Fig.3-2.

2) Comparison of the Results of MARC and ABAQUS

Model A was adopted for the constitutive equation of rubber. The results of MARC and ABAQUS were compared, and they show good agreement [Fig.3-3].

3) Comparison of computed and experimental results

The results of the ABAQUS code were compared with the experimental ones. Fig.3.4 shows the computed results using Mooney-Rivlin model, together with experimental ones. The agreement is good only up to medium shear strain. In Fig. 3.5, computed results using model (B) are compared with experimental ones. Numerical results were obtained up to 400% of nominal shear strain. (Horizontal displacement divided by total rubber thickness.)

The agreement is fairly good even in large strain. The computed deformation are shown in Fig. 3-6.

4) The results of compressible material model

The compressible model with constant bulk modulus were also used for the simulation of forced horizontal displacements of elastomer bearings. The bulk modulus was calculated from the value of Mooney-Rivlin constants assuming poison's ratio ν =0.498. The constitutive model(B) were adopted for shear strain. Shear forces computed using compressible and incompressible models are shown in Fig.3-7. The difference of the two model is small. In Fig.

3-8, the computed vertical displacements using both models are shown together.

Table-1 Type of elements

	ABAQUS	MARC
Steel	C3D8R	7
Rubber	C3D8 C3D8H	84

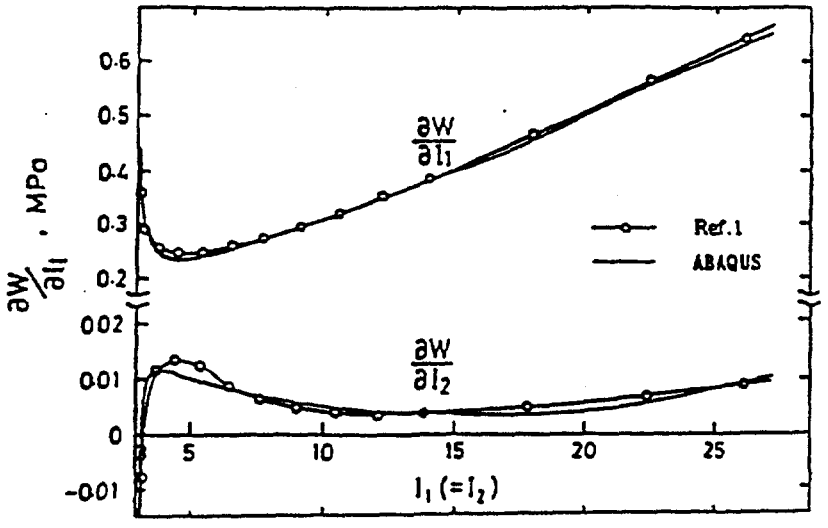

Fig.3-1 Relationship between $I_1(=I_2)$ and $\partial W/\partial I_1$, $\partial W/\partial I_2$

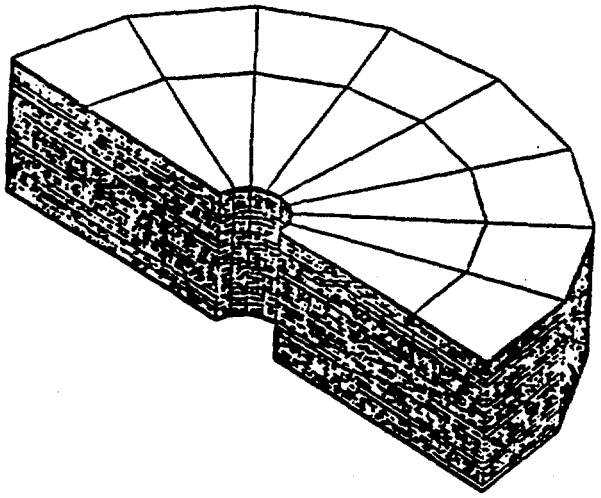

Fig.3-2 FEM mesh

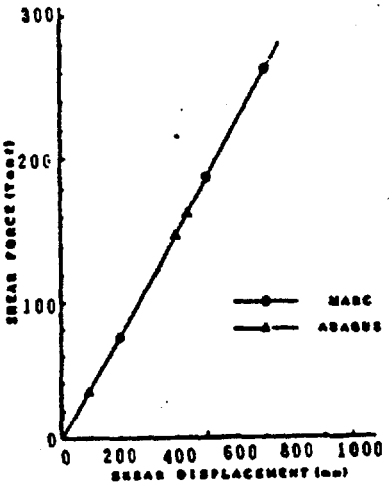

Fig.3-3 Relationship between shear force and shear displacement (Comparison of ABAQUS and MARC

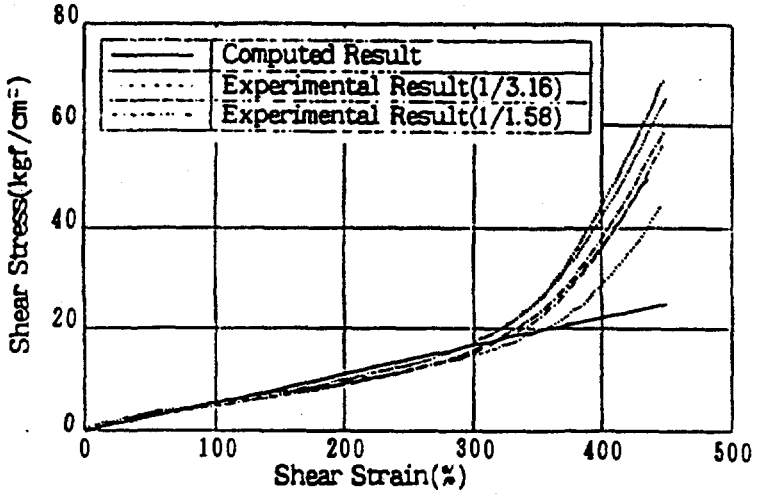

Fig.3-4 Comparison of computed results using Mooney-Rivlin model and experimental results

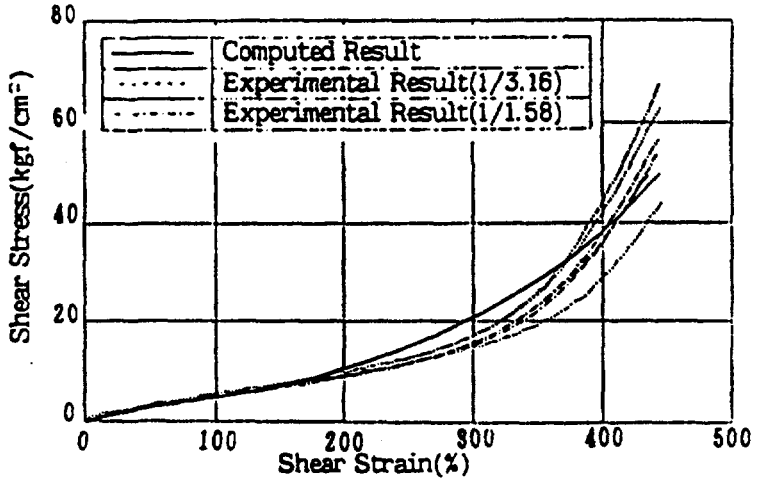

Fig.3-5 Comparison of computed results using model (2) and experimental results

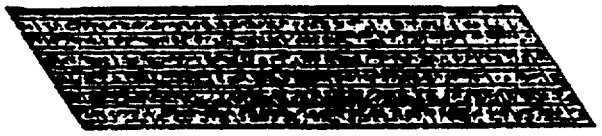

(a) Horizontal Displacement(25cm)

(b) Horizontal Displacement(50cm)

Fig.3-6 Computed deformation

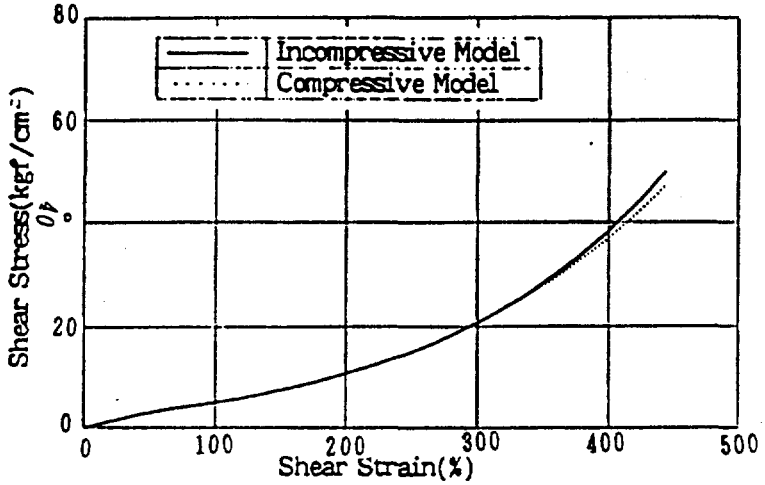

Fig.3-7 Comparison of compressive and incompressive models (horizontal direction)

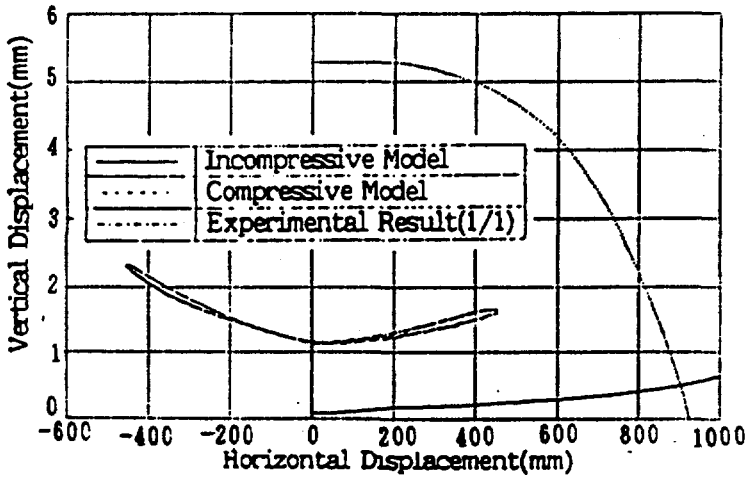

Fig.3-8 Comparison of compressive and incompressive models (vertical direction)

The difference between the computed results are large, and neither results agrees with experimental ones. The vertical displacement obtained using compressible model decrease as horizontal displacement increases. It is qualitatively contrary to experimental results.

(4) Development of Special Purpose 3-D Finite Element Code.

Special Purpose 3-D finite element code is developed for the incorporation of more general constitutive equations and interpolation functions, and remeshing of the excessively distorted elements.

1) Functional

Whereas rubber can be considered to be nearly incompressible material, compressibility of the rubber must be taken into account to evaluate vertical stiffness of elastomer bearings. The bulk stiffness of rubber is also known to be bulk strain dependent. The bulk modulus is due to the changing of interatomic spacing, where shear modulus of rubber is mainly attributable to entropy change. It is, therefore, reasonable to assume that the energy density function has the following separated form.

$$W = W_B(I_1, I_2) + W_T(I_3) \tag{3}$$

Since the bulk modulus is by far larger than shear modulus, it is still considered to be adequate to adopt mixed formulation with displacements and pressure as independent variables. The functional for mixed formulation is expressed as follows.

$$\Pi = W_s(I_1^*, I_2^*) + f(I_3)P + g(p) \tag{4}$$

where,

$I_1^* = I_1 / I_3^{1/3}$ and $I_2^* = I_2 / I_3^{2/3}$

$f(I_3) = \sqrt{I_3} - 1$

$g(p)$: complementary energy due to bulk strain

2) Constitutive equations

Model B is adopted for shear strain, and the following constitutive equation can be assued for bulk strain.

$$P = \left(\frac{C}{\sqrt{I_3} - \sqrt{I_{3e}}}\right)^n - \left(\frac{C}{1 - \sqrt{I_{3e}}}\right)^n \tag{5}$$

Were, I is ultimate deformation, and C, and N are material constants.

3) Derivation of Finite Element Scheme

Applying the variational principle on the above functional, the following weak form

equation is obtained.

$$\iiint_v t^{(1)}\,\delta\gamma^{(1)}\,dv-\iiint_v \rho_0 F^{Q}\,\delta U_Q-\iint_s \delta v_T T^{Q}\,\delta U_Q\,ds \qquad (6)$$

$$-\iiint_v f(I_3)\,\delta P\,dv-\iiint_v \frac{\partial g(p)}{\partial P}\,\delta P\,dv=0 \quad (6)$$

Where, t is 2nd Piola- Kirchhoff stress tensor, γ is Green's strain tensor, ρ is density, F is internal force, and T is surface stress.
Introducing adequate discrete interpolation function, the equations to be solved are obtained.

4) Miscellaneous

Besides the elements described in table 3-1, it is added the 27 nodes isoparametric element with 3 components of displacement at each node and 4 degree of freedom of pressure for a element. Total Lagrangian formulation is considered to be adequate for hyperelastic large deformation analysis . Remeshing algorithm is being incorporated for the analysis of extremely large deformation

4. Earthquake Response Analysis of Base Isolated Building

(1) Base Isolated Building

The base isolated building, a object of analysis is a four-story reinforced concrete building. The floor area is 1,330 m² and the weight is 2,250ton.

The seismic isolation devices consist of laminated rubber bearings and elasto-plastic steel dampers. The rubber bearing is considered to behave as a linear elastic spring up to the displacement of 200mm from the results of bearing tests conducted before installation.

The yielding displacement of the steel elasto-plastic damper is about 30mm. The periods of this building with the isolation devices are 1.4sec and 2.1sec corresponding to pre-yielding stiffness and post-yielding stiffness, respectively.

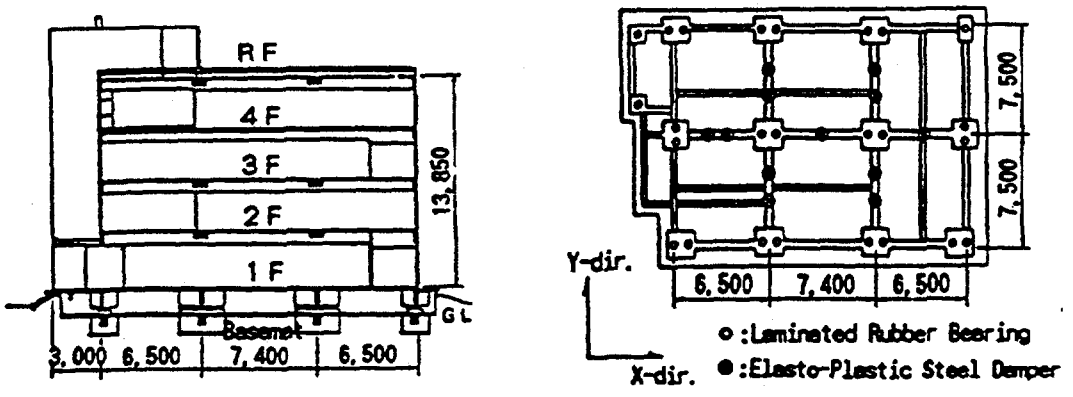

Fig.4-1 Section and plan of building

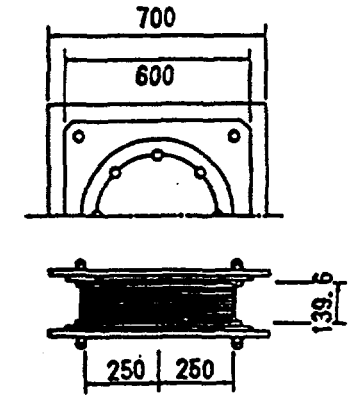

Fig. 4-2 Laminated rubber bearing

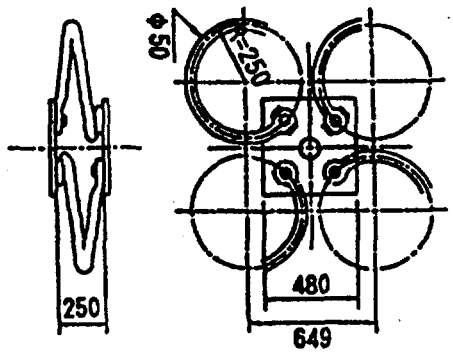

Fig. 4-3 Elasto-plastic steel damper

(2) Earthquake Response Analysis

1) Lumped Mass Model

The building above isolation devices was modeled by five lumped mass system. Isolation devices were modeled by a pair of sway and rocking springs. Fig.4-4 shows the lumped mass model. Modal analyses were used to evaluate the earthquake response of the building. The response of each mode was integrated by Newmark- β method. Model dampings were estimated from both the forced vibration test and the earthquake response observation. (Table 4-1)

Fig.4-6 shows the mode shapes obtained by the analysis. The comparison of the observed acceleration of first floor with calculated one was shown in Fig4-7

High frequency components corresponding to the second mode was excited in observed record, but excitation of high frequency components was much less in the lumped mass model. As to the acceleration of the third floor, (See Fig 4-8) the calculated result agreed well with the observed record. As to the relative displacement between the base mat and the first floor, (See Fig.4.8) the shape of calculated time history is quite similar to that of observed record.

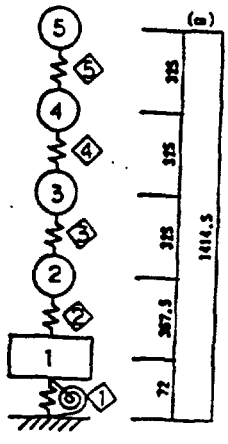

Fig.4-4 Lumped Mass Model

Analysis: Table.4.1 Analysis Condition of Lumped Mass Model

Mass or Member No.	Weight (tonf)	Stiffness (tonf/cm)	Mode No.	Damping Ratio(%)
5	408.9	1719	1	2.5
4	479.2	2718	2	0.3
3	424.0	3534	3	0.3
2	431.3	4515	4	0.3
1	502.5	71.66	5	0.3
	1.34×10^{9} (tonf·cm²)	2.05×10^{10} (tonf·cm)	6	0.3

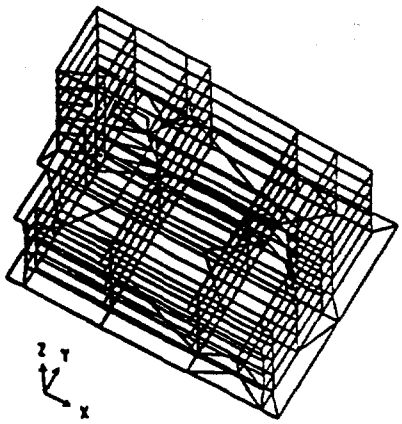

Fig.4-5 FEM Model

Table.4.2 Analysis Condition of FEM Model

Isolation Device					
Rubber Bearing				Steel Damper	
Horizontal Stiffness (tonf/cm)	Damping Ratio (%)	Vertical Stiffness (tonf/cm)	Damping Ratio (%)	Horizontal Stiffness (tonf/cm)	Damping Ratio (%)
1.61	2.5	1304	1.0	2.61	2.5

Reinforced Concrete				
Modulus of Elasticity (kgf/cm^2)	Shearing Modulus of Elasticity (kgf/cm^2)	Poisson's Ratio	Density (gf/cm^3)	Damping Ratio (%)
6.3×10^5	2.7×10^5	0.167	2.9	0.3

2) Finite Element Model

Floors and main walls were modeled by shell elements, and pillars and girders by three-dimensional beam elements. Stiffness and damping of the upper structure was estimated from both design values and the results of the forced vibration tests.

Steel dampers are modeled by horizontal shearing springs, and rubber bearings by horizontal and vertical springs.

The damping matrix was assumed to be proportional to the stiffness matrix. Fig.4-5 shows the finite element model. Analysis condition was shown in Table 4-2.

The results of finite element model is very similar to the observed records of the first floor.(See Fig.4-7)Especially excitation of the second mode is expressed well by the model. The acceleration of the third floor and the relative displacement between the first floor and the base mat calculated by this model are almost the same as those by the lumped-mass model, since these responses are dominated by the first mode.

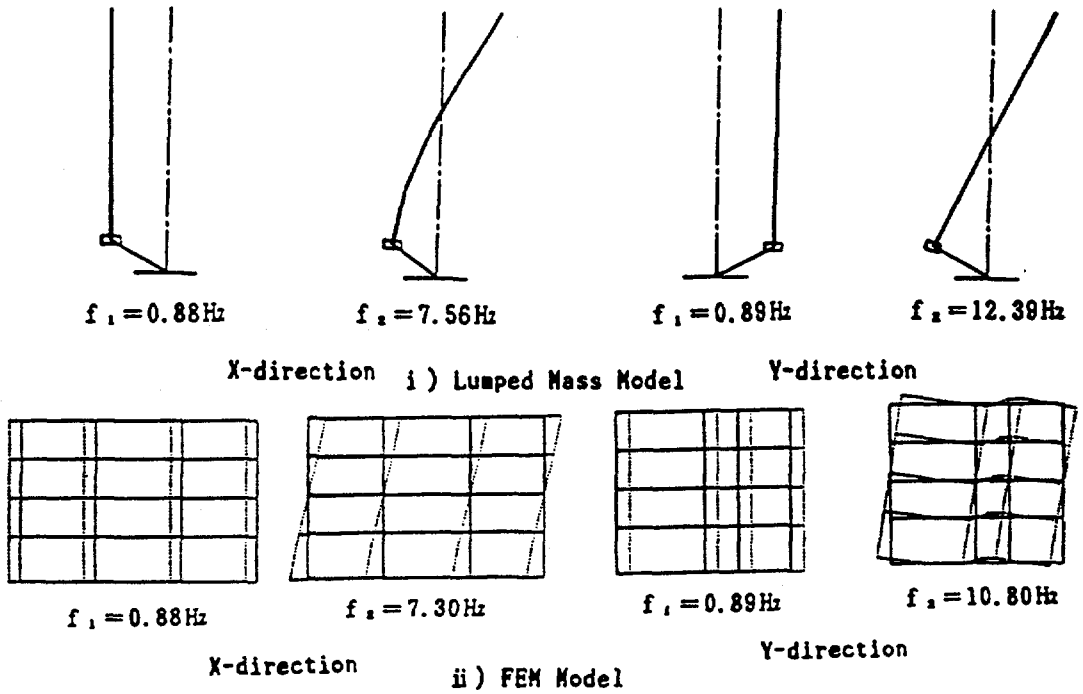

Fig.4-6 Results of Modal Analysis

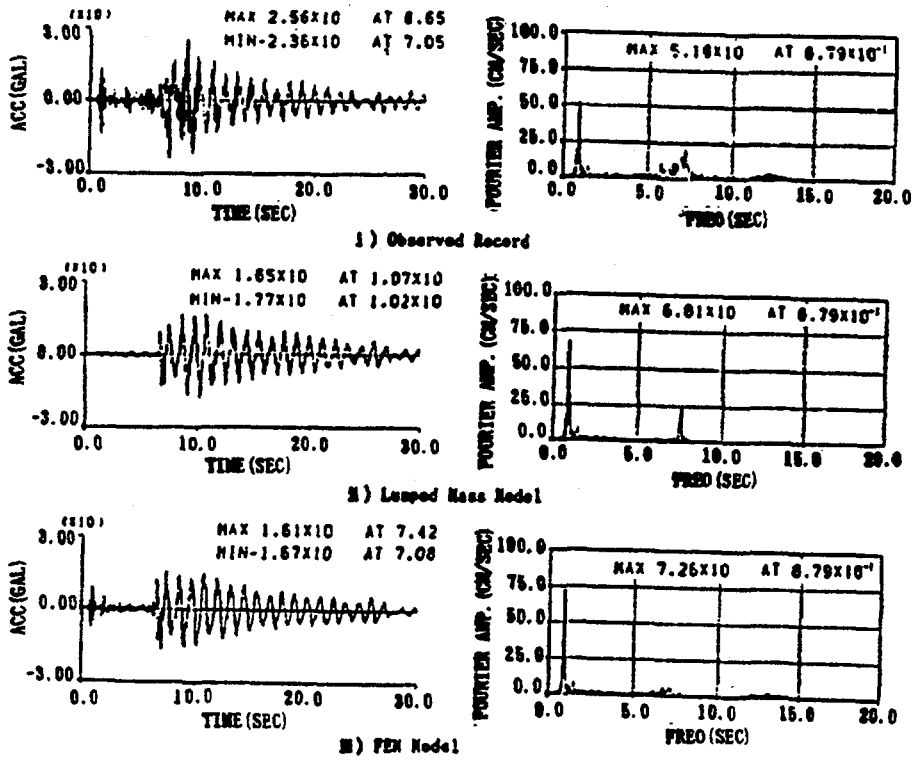

Fig.4-7 Comparison of Observed Record with Calculated Results
(Acceleration of First Floor)

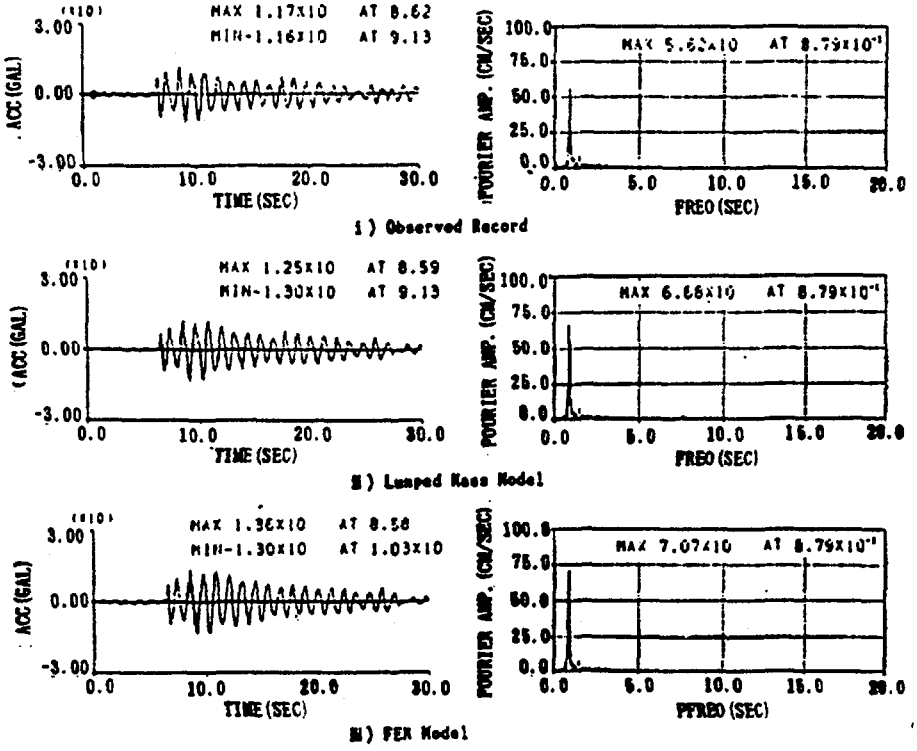

Fig.4-8 Comparison of Observed Record with Calculated Results
(Acceleration of Third Floor)

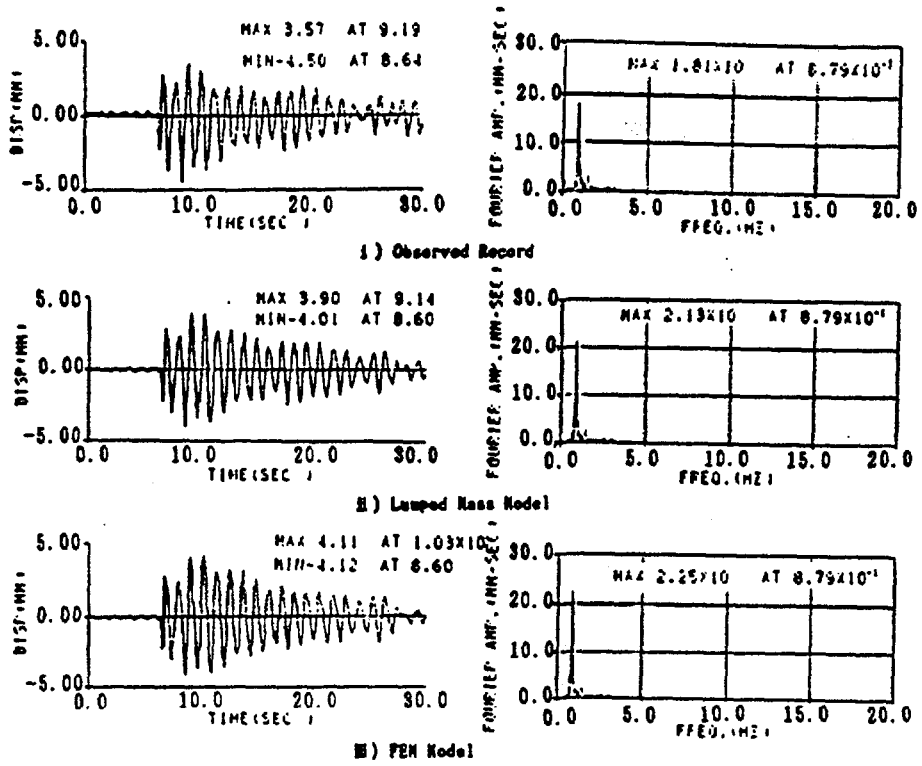

Fig.4-9 Comparison of observed record with calculated results
(Relative Displacement between Base Mat and First Floor)

3) Summary of results

Earthquake response analyses by using both lumped mass model and finite element model were carried out. The results were compared with the observed ones, and the followings are confirmed.

① lumped mass model is available to estimate the response of the upper structure and the deformation of the isolation devices, as the dynamic behavior of the base isolated building is dominated by the first mode.

② Higher mode is simulated more accurately by finite element model, and the use of this model is recommended when the effect of high frequency mode is significant.

5. Conclusions

Accurate and objective numerical modeling of behaviour of bearings are possible to simulate the shaking table tests of isolation systems.

In detailed three-dimensional analyses of single bearing, the identification of constitutive equations of rubber in bi-or tri-axial stress state is mandatary to predict the behavior of the bearing under large strain.

Simple lumped mass models are sufficient for the simulation of the earthquake response of existing base-isolated buildings. FEM model may be required to predict the floor response in high frequency range.

(Acknowledgements)

Simulations of shaking table tests are a part of research project "Verification Test of Seismic Isolation for Fast Breeder Reactor" sponsored by Ministry of International Trade and Industry, and were conducted under the guidance of Prof H. SHIBATA, Prof T. Fujita and other members of the Advisory Committee.

(References)

(1) ISHIDA,K,et,al:"Shaking Table Test on Base Isolated FBR Plant Model,Part 2 Simulation Analysis",11th SMiRT Vol,K,TOKYO(1991)

(2) SHIOJIRI,H,et,al:"Numerical Method for Analysis of Laminated Elastomer Bearings", 11th SMiRT Vol.K TOKYO(1991)

(3) MAZDA,T,et,al:"Earthquake Response Analysis of Base Isolated Building",10th SMiRT Vol,K ANAHEIM(1989)